Evaluation of a CFD Method for Aerodynamic Database Development using the Hyper-X Stack Configuration

Paresh Parikh* and Walter Engelund†
NASA Langley Research Center, Hampton, VA 23681

Sasan Armand‡ and Robert Bittner§
Swales Aerospace, Hampton, VA 23681

A computational fluid dynamic (CFD) study is performed on the Hyper-X (X-43A) Launch Vehicle stack configuration in support of the aerodynamic database generation in the transonic to hypersonic flow regime. The main aim of the study is the evaluation of a CFD method that can be used to support aerodynamic database development for similar future configurations. The CFD method uses the NASA Langley Research Center developed TetrUSS software, which is based on tetrahedral, unstructured grids. The Navier-Stokes computational method is first evaluated against a set of wind tunnel test data to gain confidence in the code's application to hypersonic Mach number flows. The evaluation includes comparison of the longitudinal stability derivatives on the complete stack configuration (which includes the X-43A/Hyper-X Research Vehicle, the launch vehicle and an adapter connecting the two), detailed surface pressure distributions at selected locations on the stack body and component (rudder, elevons) forces and moments. The CFD method is further used to predict the stack aerodynamic performance at flow conditions where no experimental data is available as well as for component loads for mechanical design and aero-elastic analyses. An excellent match between the computed and the test data over a range of flow conditions provides a computational tool that may be used for future similar hypersonic configurations with confidence.

Nomenclature and Abbreviations

α	=	Angle of attack, deg.
β	=	Angle of sideslip, deg.
C_A	=	Axial force coefficient
C_N	=	Normal force coefficient
C_m	=	Pitching moment coefficient
δ_r	=	Rudder deflection, deg.
δ_e	=	Elevon deflection, deg. (= 0.5*(δ_{Lt} + δ_{Rt}))
δ_{Lt}	=	Left elevon deflection, deg.
δ_{Rt}	=	Right elevon deflection, deg.
CNF	=	Component normal force coefficient
CHM	=	Component hinge moment coefficient
CBM	=	Component wing root bending coefficient
RV	=	Research Vehicle
HXLV	=	Hyper-X Launch Vehicle
OSC	=	Orbital Sciences Corporation

* Senior Aerospace Engineer, MS 202, Associate Fellow
† Assistant Branch Head, Vehicle Analysis Branch, MS 365, Associate Fellow
‡ Senior Engineer, MS 353X
§ Engineering Manager, MS 353X

I. Introduction

On March 27, 2004 NASA made yet another entry in the history books when its X-43A hypersonic research aircraft experiment achieved several milestones. The milestones include the first controlled accelerating flight at Mach 7 under scramjet power; the first air breathing, scramjet-powered free flight; and the first successful stage separation at high dynamic pressure of two non-axisymmetric vehicles. The flight also set a new aeronautical speed record at Mach 7 for any known aircraft powered by an air-breathing engine. This short, scramjet powered portion flight of 11-seconds showcased a culmination of years of planning, ground testing and technical work. The next X-43A flight test is planned for fall of 2004 and will test the same air breathing, scramjet powered technology at Mach 10. The complete launch system for the Hyper-X flight test experiment, referred to as the Hyper-X Launch Vehicle (HXLV) consisted of the X-43A Research Vehicle (RV) with an airframe integrated hypersonic scramjet engine, a modified, stage one Pegasus booster rocket, and an adapter connecting the two. Figure 1 shows the HXLV stack assembly being readied for a test in a hangar at NASA Dryden Flight Research Center.

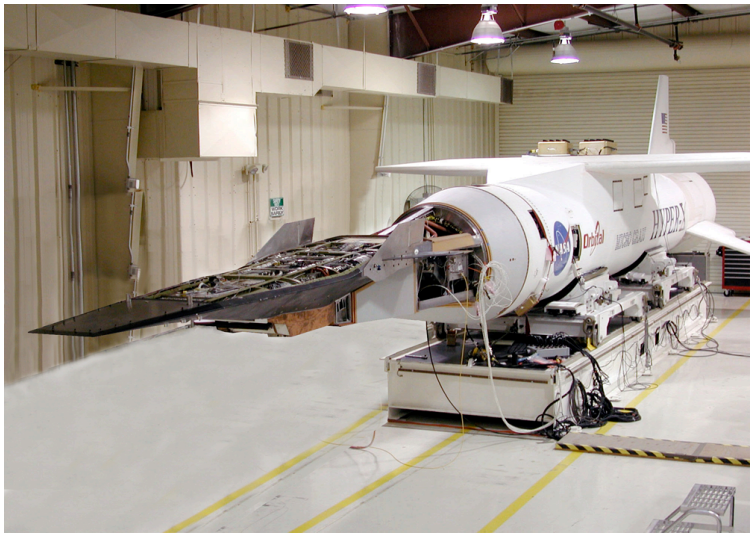

Figure 1. X-43A Stack Assembly.

A schematic of the X-43A RV, which was the focus of the entire experiment, is shown in Figure 2. The forebody inlet is designed to work as a compressor and provides the air at an appropriate amount and pressure for the airframe integrated scramjet propulsion system. The aft body of the airframe serves as an external nozzle surface, open on three sides, and is designed to optimally expand the flow. During the actual experiment, the RV was delivered to an appropriate flight altitude through the atmosphere by a rocket booster system, which was a modified stage one Pegasus vehicle designed and developed by the Orbital Sciences Corporation (OSC). The RV was connected to the booster through a specially designed adapter. The combination of the RV, the adapter and the LV is referred to as the "integrated vehicle stack" or- alternately, the Hyper-X Launch Vehicle (HXLV). The integrated vehicle was carried under the wing of a B-52B aircraft and air launched over the Western Test range off the coast of California.

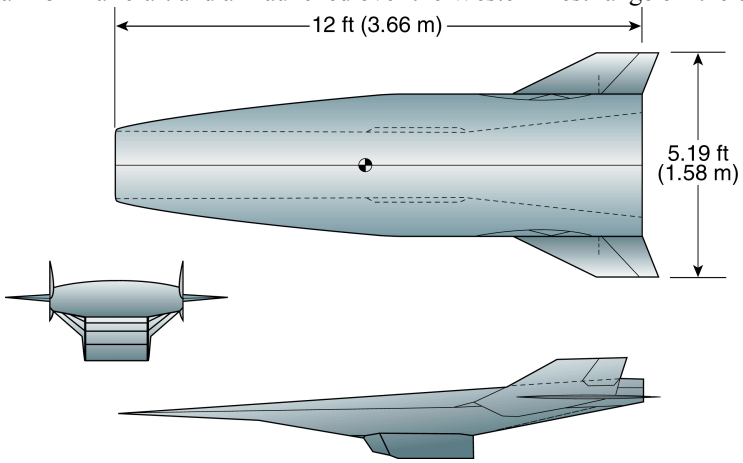

Figure 2. A Schematic of the Research Vehicle.

A representative trajectory of the X-43A flight experiment is shown in Figure 3. The B-52B carries the stack to an altitude of nearly 40,000 ft. and Mach 0.8 where the stack is released from the aircraft. After a 5-second free drop, the booster ignites and accelerates the stack to Mach 7 and at an altitude of approximately 95,000 ft. The RV is separated from the LV using a specially designed stage separation mechanism. The inlet cowl door is then opened and the 11-second hypersonic scramjet experiment is carried out followed by a controlled unpowered decent into the Pacific Ocean.

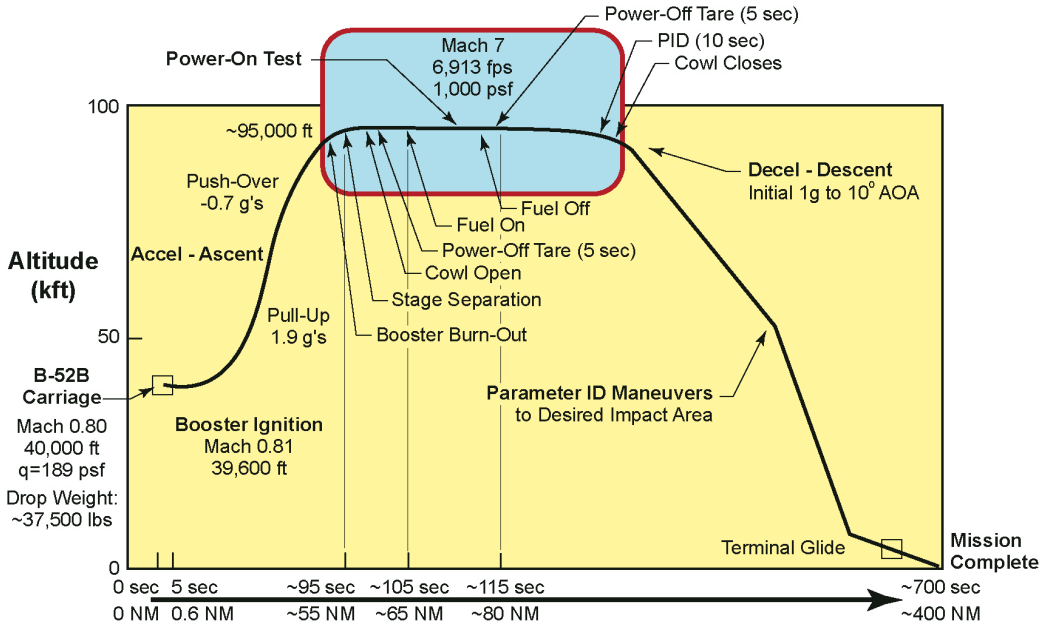

Figure 3. A Representative Flight Trajectory for the X-43A Mach 7 Experiment.

Throughout the Program, extensive efforts were made to support the development of the aerodynamic databases for all elements of the flight experiments, including the boost phase, the complex stage separation event, and the scramjet engine test at hypersonic conditions and the subsequent descent of the X-43A Research Vehicle through supersonic, transonic, and subsonic conditions prior to flight termination. Reference 1 provides details of the overall Program aerodynamic database development activities. The aerodynamic database for the HXLV configuration was developed using a combination of wind tunnel tests, Computational Fluid Dynamic (CFD) simulations and analytical engineering method analyses, and is described in further detail in Reference 2. This paper describes evaluation of a CFD procedure used to support the aerodynamic database development activities for the HXLV configuration in the Mach 0.7 to 7.0 (transonic-to-hypersonic) regime. The objectives of the study are listed first, followed by a brief description of aerodynamic database generation and the matrix of CFD solutions generated. The CFD procedure is next described and results from its evaluation and comparisons with the wind tunnel derived aerodynamic database are shown. The paper concludes with the summary of important observations learned from the study.

II. Objectives of the Present Study

The present study had three objectives: 1) To evaluate a CFD method, based on existing steady state CFD technology and unstructured-grids, for developing aerodynamic coefficients for the Hyper-X LV configuration in the transonic to hypersonic flow regimes, 2) To use this method further to fill the gaps in the experimentally obtained aerodynamic database, and 3) To estimate detailed loads on the vehicle control surfaces for mechanical design of the components and for aero-elastic analyses.

III. Aerodynamic Database for the HXLV Stack Configuration

The Hyper-X Launch Vehicle aerodynamics database, which was utilized to support the trajectory definition, guidance and control laws, and the structural and thermal protection system design requirements, was developed using a large experimental wind tunnel test effort that covered a range of flow conditions and geometric parameters.

The wind tunnel tests were supplemented, where appropriate, using CFD and analytically based engineering methods analyses. In this section we describe how the aerodynamic database was generated, its salient features and how the generated database was used.

The integrated HXLV stack aerodynamic database developed in support of the three flight tests was derived primarily from an extensive wind tunnel test campaign, consisting of 18 individual wind tunnel tests in nine separate wind tunnel test facilities. These facilities ranged in speed from low subsonic through hypersonic, and bounded the entire flight envelope for the Hyper-X Launch Vehicle boost phase of the flights up to Mach 10. These tests provided thousands of data points corresponding to a large number of flow conditions, vehicle attitude angles, and control surface positions. The subsonic, transonic, and supersonic tests were all conducted using a 6% scale stack model which, in addition to six component vehicle force and moment balance data, was instrumented to provide individual component loads including normal force, root bending and hinge moments for each of the three HXLV fins, left and right wing root bending moments, and pressure data at discrete locations over the vehicle surface.

A three percent scale HXLV model was used for hypersonic tests conducted in the NASA Langley 20-inch Mach 6 and 31-inch Mach 10 facilities. Finally, a third model at 8.33% scale, was fabricated for the stage separation testing conducted in the Arnold Engineering Development Center (AEDC) Von Karman Facility - Tunnel B at Mach 6 conditions[3].

A comprehensive CFD campaign was executed in parallel with the wind tunnel test program described above. The resulting extensive CFD solution database was utilized to further resolve experimentally obtained data at flow conditions where the wind tunnel data could not be obtained directly (e.g. Reynolds number scaling and off nominal flight conditions based on Monte Carlo simulations where direct wind tunnel data did not exist). The CFD solutions were also used to develop a detailed understanding of the flowfield structure including vortex trajectories and potential shock interactions. Finally, the CFD solution database was used to provide detailed component load distributions for mechanical and structural analysis, and to help resolve the nature of some of the experimentally derived non-linear behavior in the aerodynamic data.

One of the primary techniques utilized throughout the Hyper-X Program both to assess and reduce risk associated with the flight tests (including the HXLV booster and X-43A Research Vehicle elements) was the use of non-deterministic Monte Carlo simulation techniques in both the linear and the non-linear (6-DOF) flight simulations. In order to develop credible Monte Carlo simulation outputs, a fundamental understanding of data uncertainties used as inputs to the process must be derived. The extensive use of wind tunnel testing and CFD analysis provided a wealth of data that provided the foundation from which the derived estimates of uncertainties associated with all aerodynamic quantities were developed. This capability proved invaluable to the Program as a quantifiable means by which to understand off nominal margins and mitigate risks.

IV. Computational Procedure

All the computations presented in this paper were carried out using the NASA Langley developed TetrUSS suite of codes. TetrUSS[4] is a complete flow analysis system based on unstructured, tetrahedral grids. The Navier-Stokes grids were generated and grid quality improvements accomplished using the TetrUSS grid generation component codes VGRIDns[5] and POSTGRIDns, respectively. The flow solutions were obtained using the TetrUSS flow solver component, USM3Dns[6]. This is a three dimensional, tetrahedral, cell-centered, finite-volume, Euler and Navier-Stokes flow solver. In USM3Dns, the inviscid flux quantities are computed across each cell face using Roe's flux difference splitting (FDS). Spatial discretization is accomplished by a novel reconstruction process, which is based on an analytical formulation for computing solution gradients within tetrahedral cells. The solution is advanced to a steady state condition by an implicit backward-Euler time-stepping scheme. The Spalart-Allmaras one equation model is used to include flow turbulence effects. USM3Dns can be run in either a full viscous or a wall-function mode. However, all the calculations in the present study were performed using the full viscous mode. For all computations presented here, a callorically perfect gas assumption was made.

USM3Dns runs on massively parallel computers as well as on clusters of personal computers. Although a single processor version is available for a variety of computing platforms, the parallel version[7] is the code of choice because it enables rapid turn-around for large problems. Over the years since its first development in 1987, TetrUSS has been extensively validated on a variety of aerospace configurations in the low subsonic to low supersonic flow regimes. This is the first study where its application has been extended into hypersonic flow conditions. This has been made possible by incorporation of a special flux-splitting scheme, as described below.

A Special Flux-Splitting Scheme:

For the present study a version of USM3Dns was used that incorporates a special flux-splitting scheme based on the AUSM[8] (Advection Upstream Splitting Method) scheme. This flux scheme is known to overcome the well-known "Carbuncle Phenomenon" often associated with the application of Roe's scheme to a case with strong shock waves present in the flow field. Although the implementation of the AUSM scheme in USM3Dns has been validated before [as reported in Ref. 9], the present is the first study where it has been tested extensively over a range of flow conditions.

V. Evaluation of the CFD Method

The evaluation effort described here required 80 full Navier-Stokes solutions on the complete Hyper-X stack configuration. The CFD test matrix was selected so as to cover a range of free-stream Mach numbers, flow angles and control surface deflections. The purpose was to provide the code evaluation over as diverse a database as practical. The 80 solutions required a total of 29 separate computational grids. In VGRIDns the vehicle surface and the outer computational boundaries are represented by triangles while the volume between them is made up of tetrahedral cells. Figure 4 shows a typical surface representation used for the stack.

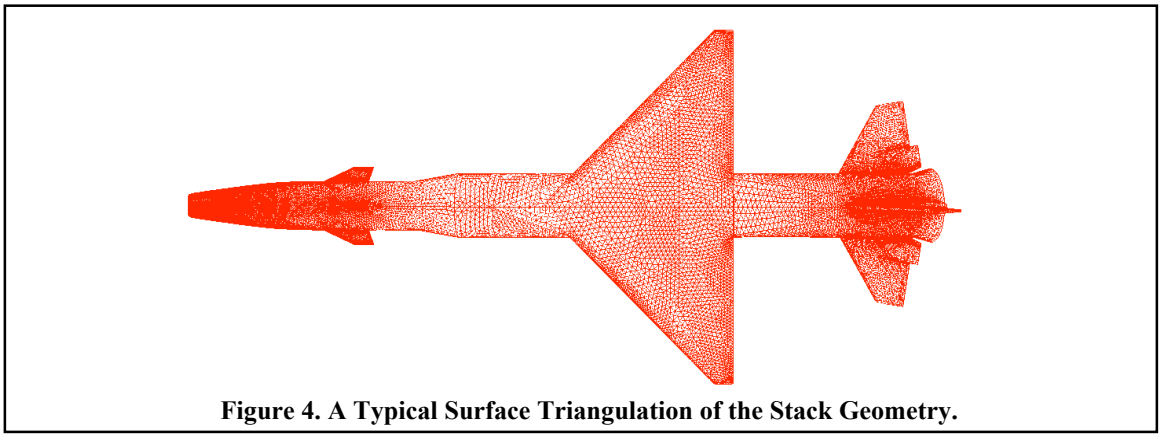

Figure 4. A Typical Surface Triangulation of the Stack Geometry.

One of the strengths of the unstructured grid technology in general, and VGRIDns in particular, is its ability in providing a user specified grid distribution on the vehicle surface as well as its distribution away from the body. This ability of the unstructured grid technology provides the desired resolution near the computational surface while at the same time, reducing the total grid size, which, in turn, directly affects the resource requirements for the computations. The surface grid spacing control ability is depicted in Figure 5, which shows a close-up of the bottom surface of the RV and a partial view of the adapter. Note the cluster of the small triangles near the expected high flow-gradient area of the vehicle leading edges and the small geometric details near the nozzle body interfaces compared to the rest of the vehicle surface.

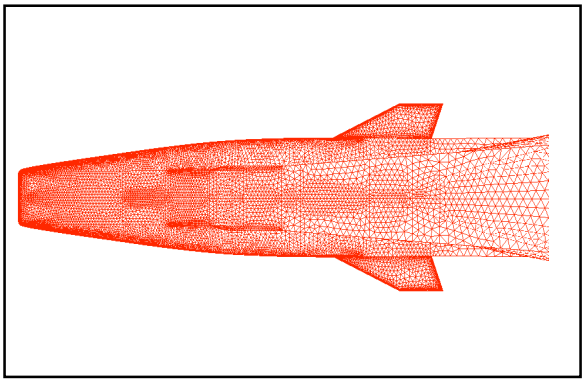

Figure 5. Surface Grid Close-Up on the bottom of the RV.

The 29 computational grids differed in size slightly on account of the differences in the LV control surface deflections. However, a typical model was made up of an average of nearly 4 million surface triangles and

approximately 10.5 million tetrahedral cells. All the grids were generated with a spacing normal to the vehicle surface corresponding to a $y^+ = 1$ suitable for a flow of a free-stream Reynolds number per foot of $15.8X10^6$. This was the average Reynolds number at which most of the wind tunnel tests were conducted on the scaled model of the HXLV stack. Although the run matrix contained several cases that were symmetrical left-to-right, for which a half-configuration could have been modeled, it was decided at the outset to use full configuration grids for all the cases in order to remove discrepancies or uncertainties due to grid sensitivities.

The CFD solutions were obtained using a multi-processor version of USM3Dns running either on a 48-processor Pentium-4 cluster or a 64-processor SGI Origin 2000 cluster. An attempt was made to execute each CFD case for the number of iterations required for a satisfactory convergence to a steady state. This requirement resulted in an average of 4500 flow iterations at about 20 hours of wall-clock time using 48 processors for each run. Of course the actual number of iterations required to obtain steady state solution were dependent on many factors; chief among them being the flow initialization and free-stream flow conditions. It may also be noted that, although the flow solver is spatially accurate to 2nd order, some of the high Mach number cases had convergence problems while doing 2nd order accurate spatial calculations. For such cases a 1st order spatial accuracy was used. Table 1 lists the ranges of parameters covered by the present study. The 80 CFD cases covered a combination of these parameters.

Quantity	Range
Mach Number	1.1, 1.28, 1.4, 2.8, 4.6, 6.0, 7.0
Angle of Attack (α), deg.	-2.84 to 12.35
Angle of Side Slip (β), deg.	-3.0, 0.0, 3.0
Rudder Deflections (δ_r), deg.	-5.0, 0.0, 5.0
Elevon Deflections, (δ_{Lt}, δ_{Rt}) deg	-22.5, -20.0, -17.5, -15.0, -12.5, -10.0, -7.5, 0.0, 2.5, 5.0, 7.5

Table 1. CFD Run Matrix- Range of Parameters

CFD Experiment Comparison:

As a first evaluation of the CFD method, the longitudinal coefficients of normal force (C_N), axial force (C_A) and pitching moment (C_m) were compared between the CFD and the experiments at several free-stream Mach numbers. For each case, the coefficients were calculated from the converged CFD solutions by integrating the surface pressures on all vehicle surfaces including the sheer component. However, for the axial force calculations, the contribution from the LV rocket jet exhaust plane was excluded. This was done for a true comparison against the un-powered wind-tunnel experimental data, which had a backpressure correction applied to account for the presence of the model sting.

In Figure 6, the five CFD cases shown correspond to three different elevon deflections, δ_e, on the HXLV: three angles of attack for δ_e of -12.5^0 and one each for δ_e of -17.5^0 and -7.5^0. The reason for selecting these five cases for CFD was to cover the nominal point on the trajectory and small perturbations on either side in both alpha and the elevon deflection. It may be noted that in this and similar subsequent figures which include the OSC data, the vertical scale is suppressed due to the proprietary nature of the data. However, to aid a reader, a range is shown that depicts the increment in the coefficient plotted between two successive tic marks on the vertical axis. As can be seen, all three longitudinal coefficients agree very well with the experimental data. The excellent agreement between the CFD and the database attest to the predictive capability of the CFD method. This is not a surprise as the CFD method used here has been extensively validated for transonic flows. The excellent comparison, however, does show the adequacy of the grid for the purpose for which it is used. Figure 7 shows a similar comparison at a free-stream Mach number of 2.8. For this case, the nominal point on the trajectory is at an angle of attack equal to 5.13^0 and a δ_e of -7.5^0. For this case also the axial and the normal force are predicted well, while the pitching moment is slightly over predicted. Comparing these results with the pitching moment for M=1.1, please note the small scale of the vertical axis in Figure 7 which exaggerates the differences.

Data in next two figures show similar comparisons at two other points along the trajectory, at Mach number of 4.6 and 6.0, respectively. These figures show a relatively good agreement and the trends are well predicted. However, the results of these cases do not match the experimental data as accurately as the ones for the transonic cases. Several reasons can be attributed to this; the first being that most of these high Mach number cases could not be converged to 2nd order accurate spatial solution. The transonic cases, on the other hand, were converged using the 2nd order accurate solution. This lack of higher order convergence may be attributed to inadequacy of the size of the computational grid. A grid convergence study, limited in scope to a few transonic and supersonic Mach number cases was performed in the beginning of the program, and results from this study were used in determining the grid size for the subsequent CFD runs. The higher Mach number cases reported here were run later in the program, and a further grid refinement could not be performed due to the tight time constraint imposed by the programmatic

requirements of completing all the 80 Navier-Stokes runs in a short time of 90 to 100 days. It should also be noted that the error bounds on experimental data were not available at the time, and continue to be proprietary. Nonetheless, the CFD data were considered adequately accurate for the purpose of this project.

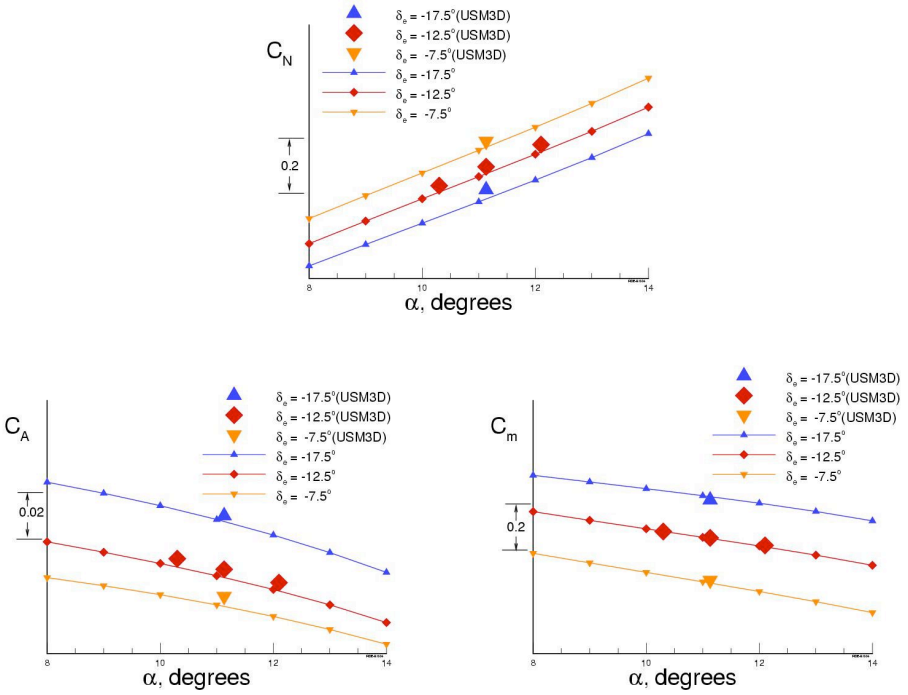

Figure 6. CFD-Data Comparison of Longitudinal Coefficients at Mach number 1.1.

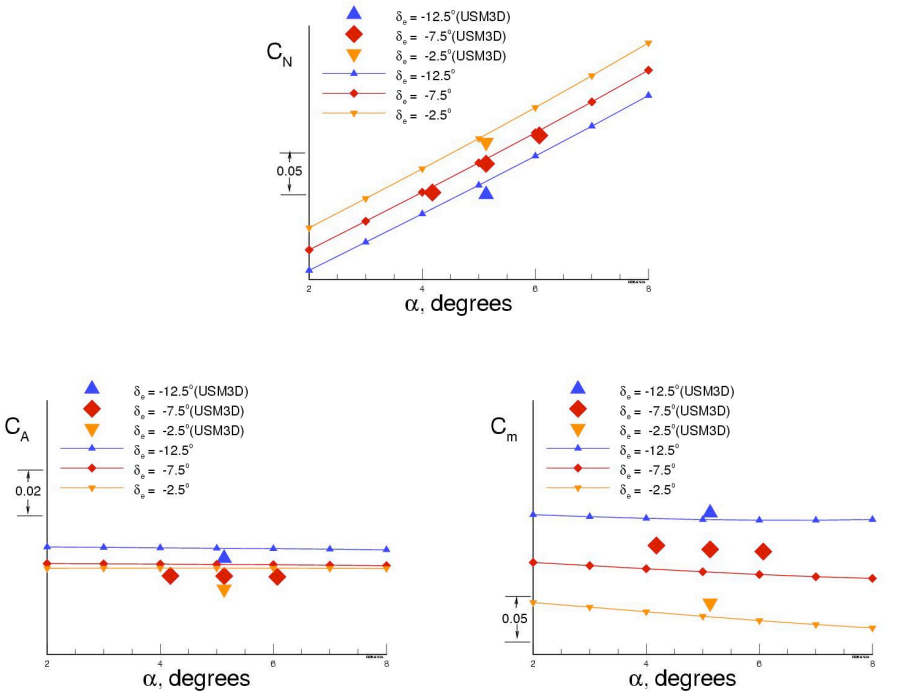

Figure 7: CFD-Data Comparison of Longitudinal Coefficients at Mach number 2.8.

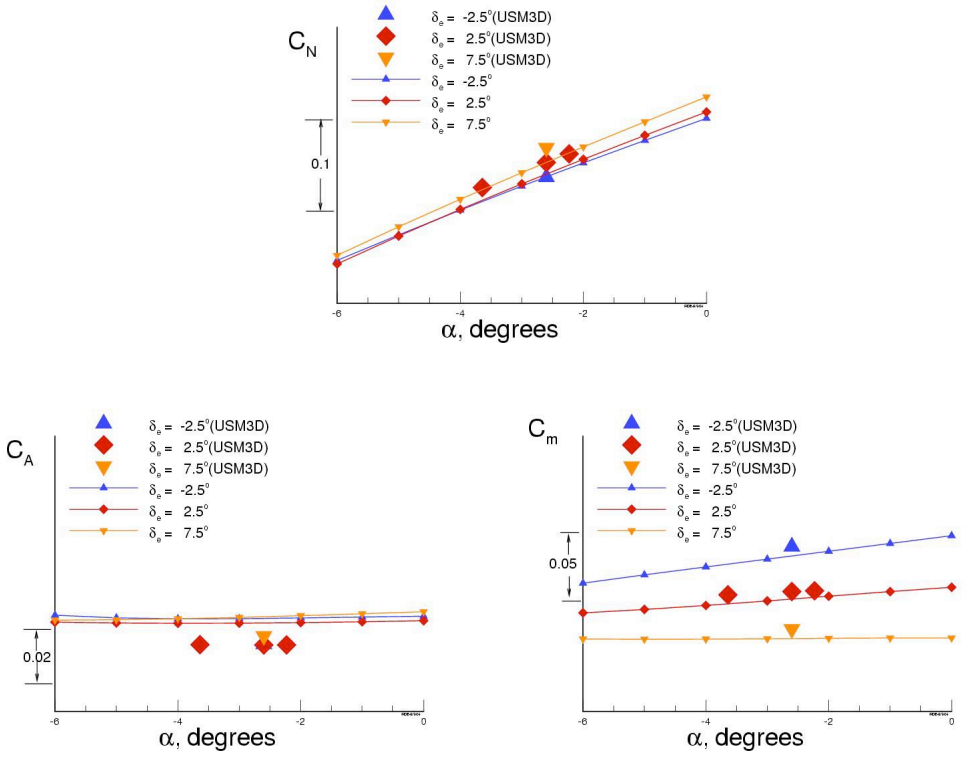

Figure 8. CFD-Data Comparison of Longitudinal Coefficients at Mach number 4.6.

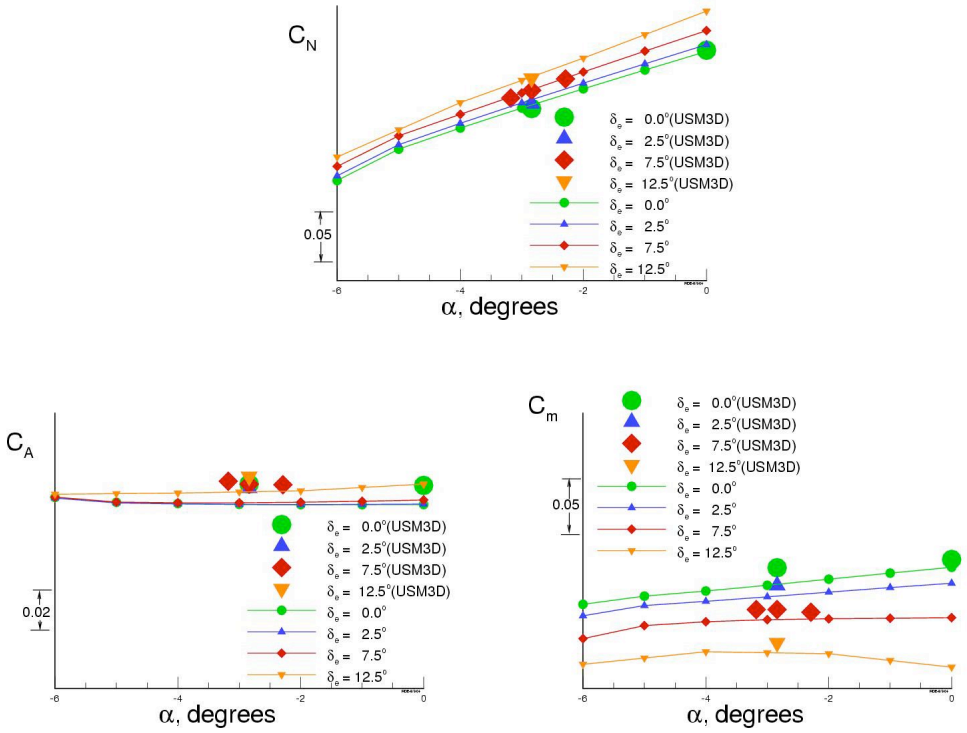

Figure 9. CFD-Data Comparison of Longitudinal Coefficients at Mach number 6.0.

Comparison of Surface Pressures:

While the computational method was reasonably successful in that the integrated forces and moments for a range of flow conditions were predicted with accuracy, the next level of evaluation was needed to develop confidence in the CFD method's predictive accuracy. As mentioned earlier, surface pressures were measured during several of the tests conducted using the 6% HXLV model. A schematic of the wing fillet with pressure tap locations, is shown in Figure 10. The pressure tap numbers increase in the stream-wise direction. Please note that on the wind tunnel model all, except tap number 17, were on the port side. Tap number 17 was on the starboard side at a location, which mirrored number 16 on the port side.

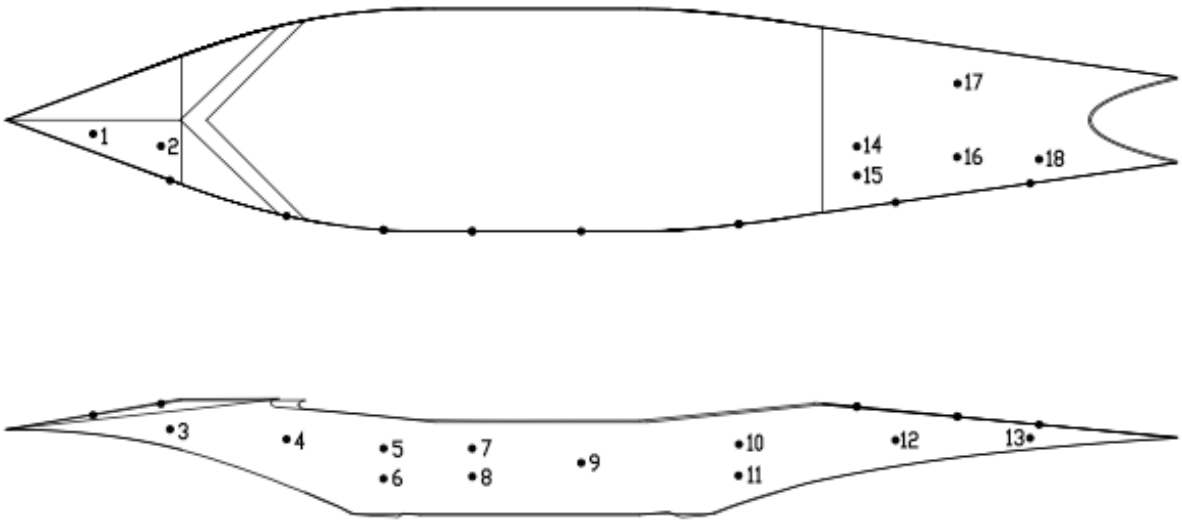

Figure 10. Pressure Tap Locations on LV Wing Fillet.

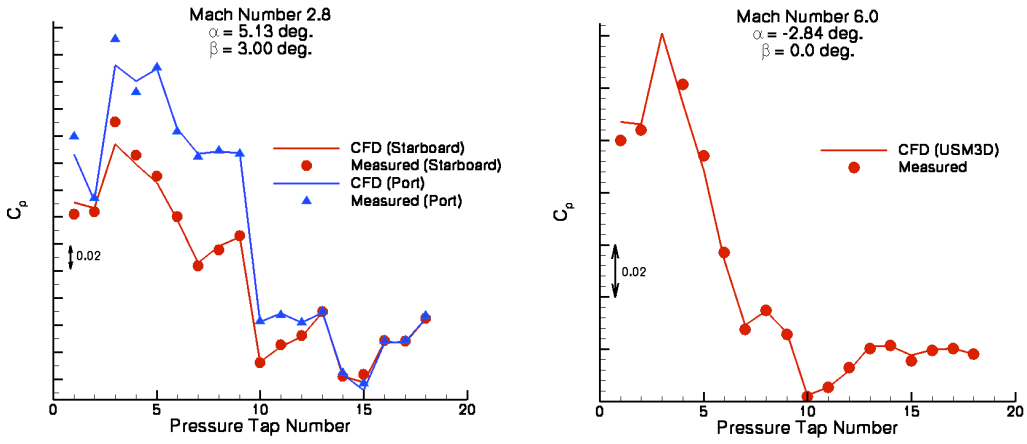

Figure 11. CFD-Data Comparison of LV Wing Fillet Pressures.

The CFD-experiment comparison is shown in Figure 11 for two Mach number; one in the supersonic and one in the hypersonic range. The CFD pressures shown were interpolated at the pressure tap locations by first identifying the surface triangle of the computational grid that surrounded the tap in question. The pressure at the tap location was then arrived at by a weighted interpolation from the three nodes of the triangle. For the figure on the left, at □ =

3.0 deg, the starboard side of the pressures are actually for the wind tunnel model at –3.00 deg. As can be seen, the CFD method accurately predicted the detailed pressures at both the flow conditions shown. Although not shown, it may be noted that, the predicted pressures matched equally well for a wide range of flow conditions, and thus attests to the accurate predictive capability of the CFD method.

Comparison of Component Forces:

As yet another test of the accuracy of the CFD method, the computed forces and moments on the LV control surfaces (elevons and rudder) were compared against those measured during the wind tunnel test. As mentioned earlier, the wind tunnel model was instrumented to provide individual component loads including normal force, root bending and hinge moments for each of the three HXLV fins. A typical comparison of component loads is shown in figure 12. Both the rudder normal force and root bending moment coefficients are predicted very well.

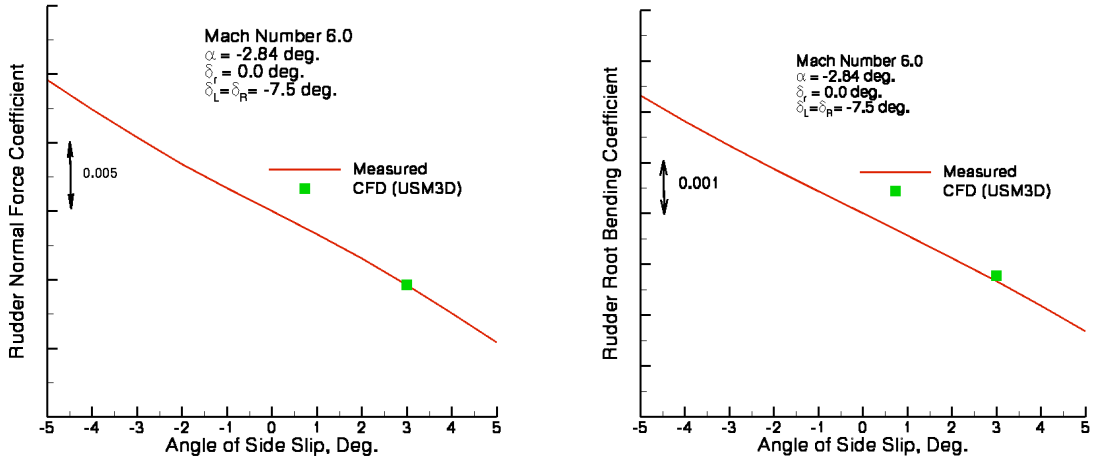

Figure 12. Comparison of Component Forces

With the comparison exercises yielding confidence in the ability of the CFD to predict the aerodynamic pressures and forces reasonably well, the method was next applied to fill in the gaps in the experimental data, to explain or dispute experimentally observed anomalies and for obtaining detailed surface pressures for aeroelastic analyses. These applications were too numerous to detail here, suffice it to state that in most all cases the CFD method equaled or exceeded the expectations, thus establishing it as a viable tool for such exercises in the future.

VI. Post Flight Analysis

Following the highly successful second Hyper-X flight test, in which the HXLV booster delivered the X-43A Hyper-X Research Vehicle to the Mach 7 scramjet engine test condition, detailed comparisons were made with the preflight models (both experimental and CFD derived) and flight derived data. Although the bulk of the HXLV booster performance data remains proprietary with the Orbital Sciences Corporation, it is fair to say that the ground based models, including the preflight CFD predictions, did an admirable job in predicting the aerodynamic characteristics, and in general the agreement with flight data was very good to excellent. The Hyper-X Program is pressing ahead in preparation for the third flight, to be conducted at Mach 10 conditions in the fall of 2004, and is utilizing the same strategies for CFD analysis and wind tunnel derived database development that proved so successful in the second flight.

VII. Conclusions

A CFD method, based on unstructured grids is evaluated against a set of experimental data for the Hyper-X Launch Vehicle stack configuration in the transonic to low hypersonic flow regime. The CFD method accurately predicts not only the integrated forces and moments, but also surface pressures and component loads. Based on the confidence generated during this exercise, the method is presently used for filling gaps in the aerodynamic database for the third flight of the Hyper-X experiment, scheduled for the fall of 2004.

VIII. Acknowledgement

The authors would like to thank Dr. Edward Parlette of ViGYAN, Inc. for his timely help during the daunting grid generation task for the present work. The help provided by the NAS computer system staff at NASA Ames in assigning priority for some of the computational work is gratefully appreciated.

References

[1] Engelund, W. C., Holland, S. D., Cockrell, C., E., Bittner, R. D.: "Aerodynamic Database Development for the Hyper-X Airframe Integrated Scramjet Propulsion Experiment." *Journal of Spacecraft and Rockets*, **Vol. 38, No. 6**, pp. 803-810, Nov-Dec, 2001.

[2]Bermudez, L.M., Gladden, R.D., Jeffries, M.S., McMillan, D.L. et al, "Aerodynamic Characterization of the Hyper-X Launch Vehicle", AIAA-2003-7074, December 2003.

[3]Woods, W.C., Holland, S.C, and DiFulvio, M., "Hyper-X Stage Separation Wind-Tunnel Test Program", *Journal of Spacecraft and Rockets,* Vol. 38, No. 6, November-December 2001.

[4]Frink, N.T., Pirzadeh, S., Parikh, P., Pandya, M.J., and Bhat, M.K., "The NASA Tetrahedral Unstructured Software System (TetrUSS)", ***The Aeronautical Journal***, Vol. 104, No. 1040, October 2000, pp. 491-499.

[5]Pirzadeh, S., "Three-Dimensional Unstructured Viscous Grids by the Advancing Layers Method", AIAA Journal, Vol. 34, No. 1, January 1996, pp. 43-49.

[6]Frink, N.T., "Tetrahedral Unstructured Navier-Stokes Method for Turbulent Flows", AIAA Journal, Vol. 36, No. 11, November 1998, pp. 1975-1982.

[7]Bhat, M. K. and Parikh, P., "Parallel Implementation of an Unstructured Grid-Based Navier-Stokes Solver",AIAA-99-0663, January 1999.

[8]Wada, Y. and Meng-Sing, L., "An accurate and Robust Flux Splitting Scheme for Shock and Contact Discontinuities", *SIAM Journal of Scientific Computations*, Vol. 18, No. 3, pp. 633-657, May 1997.

[9]Bobskill, G. J, Parikh, P., Prabhu R. K. and Tyler, E.D., "Aerodynamic Database Development for Mars Smart Lander Vehicle Configurations", AIAA-2002-4411, August 2002. Accepted for publication in *Journal of Spacecrafts and Rockets.*